愛知工業大学研究報告
第２９号　　平成６年

High Capacity of Differentially Detected π/4-shifted DQPSK with Narrowing Occupied Bandwidth based on Short Time DFT

Short Time DFTによる狭帯域化技術を用いた差分検波π/4-shifted DQPSKの大容量化

岸　政七†
Masahichi KISHI

ABSTRACT *This paper presents the narrowing bandwidth of π/4-shifted DQPSK, which has previously achieved using raised cosine filter, at 1.62bit/Hz efficiency, with based on the Nyquist Kaiser filter and generalized short time DFT (ST gDFT) demodulator. Such degradations as caused from Gaussian thermal and fading click noise are desmeared through ST gDFT to improve efficiency more than 1.80bit/Hz.*

1. INTRODUCTION

Narrowing bandwidth of the modulated signals is one of the promising solution to using finite radio frequency resource effectively. The Nyquist filter has previously discussed in narrowing frequency occupancy over π/4-shifted DQPSK transmission system in order to perform such high efficiency as 1.62bit/Hz. [1,2]

In addition to these discussion about matched filters, generalized short time DFT (ST gDFT) is adopted to the demodulator to make the efficiency more than 1.80bit/Hz on the bases of excluding phase distortion in signal processing. In genius, ST gDFT posses function of eliminating inter symbol interference since Nyquist Kaiser function is employed to improve frequency resolution by manipulating plural frame data. Randomness caused from Gaussian thermal and fading click noise is desmeared with convolution over such long period data by Nyquist Kaiser.

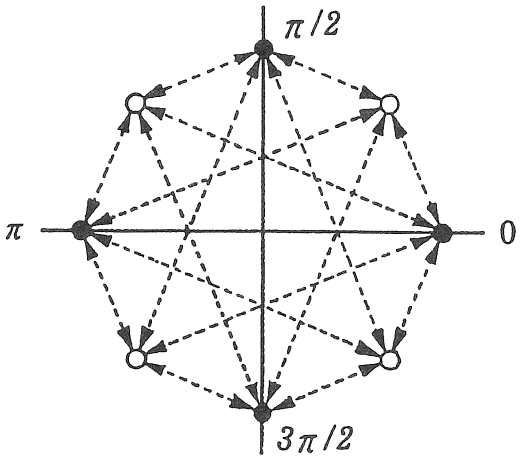

Fig.1 π/4-shifted DQPSK Citation.

2. MODULATION

The citation employed in this discussion for the π/4-shifted DQPSK is shown in fig.1. The citation consists of eight phases. These eight phases are formed by superposing two QPSK citations offset by π/4radian relative to each

† 愛知工業大学　情報通信工学科（豊田市）

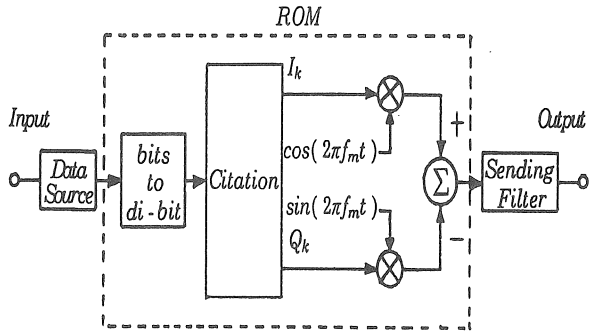

Fig.2 Block diagram of the π/4-shifted DQPSK modulator based on ROM reading.

other.

Figure 2 shows the block diagram of the $\pi/4$-shifted DQPSK modulator employed in the experiment based on the ROM reading. The composition of ROM used for the modulator is shown in fig.3. A wave data for one cycle of the carrier signal is memorized beforhand in ROM. The phase of transmit signal readout is decided by the pointer which moves on the citation to carry I_k and Q_k of baseband signals. The pointer moves alternately among black points or white points. As a result, symbols have a relative phase difference that is one of four angles, $\pm\pi/4$and $\pm 3\pi/4$ radian.

3. FILTER

The condition that the inter symbol interference after reception equalization becomes a zero is very important for design of the base transmission system. Nyquist function which is ideal as low pass filter is considered to match this condition. However, there exists such problem on developing stages as Nyquist function being infinite in filter length and robustness for synchronization being week in some deviations.

Therefore, in the conventional system, raise cosine(RC) filter is employed as a roll-off filter.

$$R(p) = \frac{\sin \pi p/N}{\pi p/N} \cdot \frac{\cos \alpha\pi p/N}{1-(\alpha p/N)^2} \qquad (1)$$

Equation 1 is the typical filter designed for remaining symmetry on the frequency domain according to Nyquist.[3] Equation 2 shows Nyquist Kaiser window as another design for RC filter in which the Nyquist function is modified by weighting Kaiser windows.

$$h(p) = N(u)\, K(\beta, v), \qquad (2)$$

$$u = \frac{p}{mN}, \quad -1 \le u \le 1,$$

here,

$$N(u) = \sin \pi u / u, \quad u = \frac{\pi p}{N} \qquad (3)$$

$$K(\beta, v) = \frac{I_0\left\{\beta\sqrt{1-v^2}\right\}}{I_0(\beta)}, \qquad (4)$$

$$v = \frac{p}{mN}, \quad |v| \le 1$$

where $I_0(*)$ is the modified 0_{th} order first kind Bessel, β is arbitrary parameter.

It is easy to recognized that Nyquist Kaiser function is able to improve the characteristic of preventing inter symbol interference because Nyquist function maintains the condition of nullity at zero every N sampling clock according to weighting Nyquist by Kaiser function on the time domain. In addition to improvement of inter symbol interference, this Nyquist Kaiser desmears impulsive fading noise to improve the signal to noise ratio because it executes over plural frames through signal processing. This becomes to the second merits introduced from Nyquist Kaiser window if its

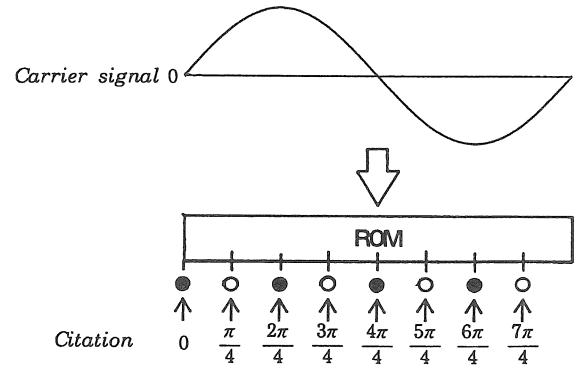

Fig.3 Composition of ROM used for the modulator.

characteristics is set to equal that of RC filters by adjusting parameter β. Desmearing effect is obtained from the Nyquist Kaiser for all value of β because the ensemble average of the Nyquist Kaiser function becomes unity over the period from 0to N. Therefore, such random noise as thermal and fading clicks intend to cancel out through superposing noise over plural frames of the Nyquist window. Consequently, noise over radio channels are desmeared to improve CNR or BER through employing the Nyquist Kaiser as match filters.

Figure 4 shows the relationship between $\alpha$of RC filter and $\beta$of Nyquist Kaiser when each impulse response coincides with each other over all frames as shown in fig.5 as the frame number $2m$ being taken as a parameter. By adjusting βvalue, the attenuation of the impulse response is matched to give the same response on the time domain. The dotted curve shows the impulse response for RC filter of $\alpha = 0.5$ and solid curve shows that of Nyquist Kaiser filter of $\beta = 8.560$. Those are almost equal on the time domain as shown in fig.5.

Figure 6 shows frequency responses for RC filter by dotted curve and for Nyquist Kaiser by solid curve on the same conditions mentioned aboves. It is shown clearly in the same figure that Nyquist Kaiser filter is superior than RC filter by more than 32dB in eliminating frequency component on the stopband. It may be possible to get followings that Nyquist Kaiser is more suitable for narrowing occupied bandwidth on the radio channel than the existing RC filter.

4. CHANNELS

Two types of channels are considered. One is static channel, a flat Rayleigh fading channels assumes White Gaussian noise as additive interference. The other is a dynamic channels, in which a fading sim-

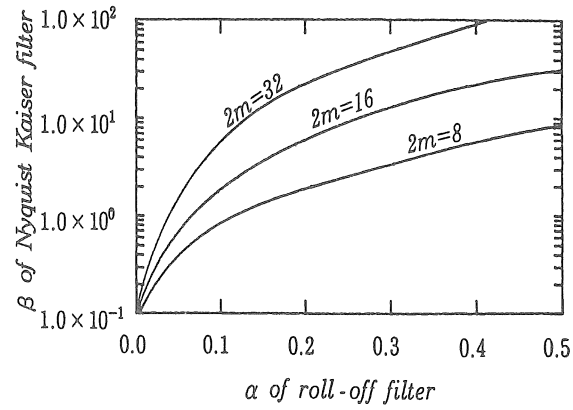

Fig.4 Relationship between α of RC and β of Nyquist Kaiser filter for the same impulse response.

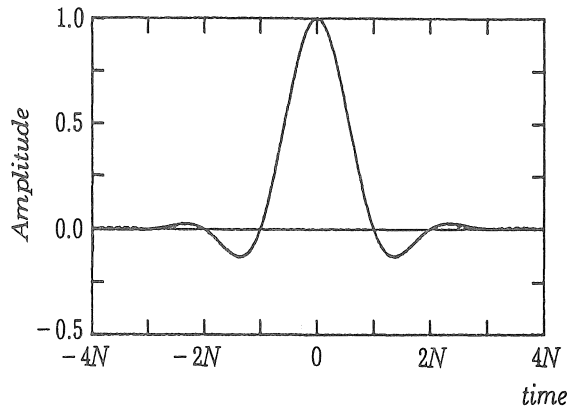

Fig.5 Impulse responses for Rc of α=0.5 plotted by dotted curve and for Nyquist Kaiser filter by solid curve.

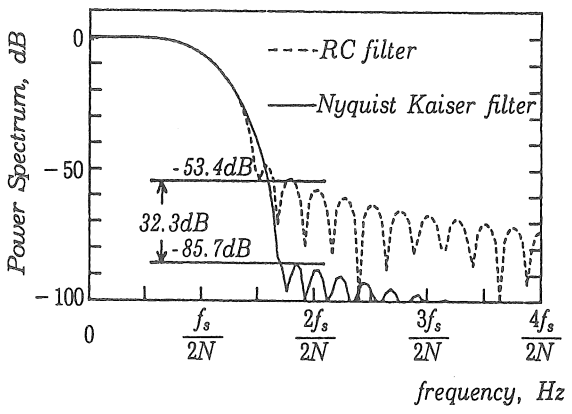

Fig.6 Frequency response for the Nyquist Kaiser filter, β= 8.560, illustrated by solid curve and for the existing RC filter by dotted curve, α=0.5.

ulator is employed based on two ray model in addition to the White Gaussian noise.

The fading simulator operates on narrow-band frequency bandwidth at IF, here fading pitch is assumed, for example, 40 Hz. As shown in fig.7 for power variation of ST DFT fading simulator is observed to match well to practical multipath fading. [4]

5.DEMODULATOR

Figure 8 is a block diagram of the demodulator which operates for IF input signals. $\pi/4$-shifted DQPSK baseband signal I_k and Q_k are analyzed to decode k_{th} di-bit carried over k_{th} symbol period by differentiating ϕ_k of the current period from $\phi_{k-1}$of the previous period carrier phase. Carrier frequency f_m of $I_k$and Q_k and the symbol period are adaptively adjusted by symbol period and carrier frequency estimation adjuster (SCA) to yield maximum power ratio of $I_k$to Q_k. Receiving filter is the same to the roll-off filter at sending site under assumption of the distortion over radio frequency being reasonably small.

$\pi/4$-shifted DQPSK signal $x(t)$is given as

$$x(t) = I_k \cos(2\pi f_m t) - Q_k \sin(2\pi f_m t) \quad (5)$$

here,

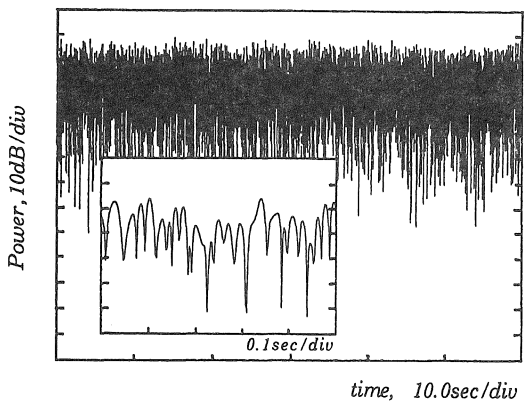

Fig.7 Power variation of ST DFT fading noise simulator.

$(N-1)\tau \le t < N\tau$,

$\tau$is a reciprocal number of the sampling frequency.

If these exist phase error φin the carrier frequency extracted in the demodulator, receiving $\widetilde{I_k}$, $\widetilde{Q_k}$is given

$$\begin{aligned}\widetilde{I_k} &= \frac{1}{T}\int_0^T \{I_k\cos(2\pi f_m t) - Q_k \sin(2\pi f_m t)\}\cdot \\ &\quad \cos(2\pi f_m t + \varphi)dt \\ &= \frac{I_k}{2T}\int_0^T \{\cos(4\pi f_m t + \varphi) + \cos\varphi\}dt \\ &\quad - \frac{Q_k}{2T}\int_0^T \{\sin(4\pi f_m t + \varphi) - \sin\varphi\}dt \\ &= \frac{I_k}{2}\cos\varphi + \frac{Q_k}{2}\cos\varphi,\end{aligned} \quad (6)$$

here, $T = 2\pi\tau$. $\widetilde{Q}_k$is calculated in similar to the above equation. That is,

$$\begin{aligned}\widetilde{Q_k} &= \frac{1}{T}\int_0^T \{I_k\cos(2\pi f_m t) - Q_k \sin(2\pi f_m t)\}\cdot \\ &\quad \sin(2\pi f_m t + \varphi)dt \\ &= \frac{I_k}{2}\sin\varphi + \frac{Q_k}{2}\cos\varphi\end{aligned} \quad (7)$$

As shown eqs.6 and 7, the maximum power ratio of $\widetilde{I_k}$ to $\widetilde{Q_k}$is given by $\varphi = 0$. The phase of extracted carrier becomes to synchronize with the carrier of $x(t)$included in IF band.

$$\lim_{\varphi\to 0}\widetilde{I_k} = \frac{1}{2}I_k, \quad \lim_{\varphi\to 0}\widetilde{Q_k} = \frac{1}{2}Q_k \quad (8)$$

As shown in citation of $\pi/4$-shifted DQPSK, 2bits is precisely decoded by 2π modulus correction given by ref.1 where the carrier phase is exactly extracted from receiving signal over corresponding symbol period.

Demodulation given by eqs.6 and 7 for continuous signal $x(t)$is equivalently executed by discrete Fourier transform (DFT) for sampled data $x(n)$, here $n$is sampling clock. Dotted line in fig.9 means the operand over data stream to show the frame of DFT.

When the first sub-channel of the DFT is employed to execute eqs.6 and 7, the al-

location of the first sub - channel is illustrated over phase plane as shown in fig.10 by solid lines. It is not necessary to restrict the allocation to the first sub - channel of DFT, it is for ease of discussion without any loss of generality to employ 1 st sub - channel of DFT in the followings.

Center frequency of the first sub - channel is set to be f_m on the domain $(f_m/2,\ 3f_m/2)$, because the bandwidth of each sub - channel is chosen to be f_m in the meanings of frequency resolution. When the sampling frequency f_s is Nf_m, I_k and Q_k are literally given by eqs.6 and 7 with bases on that the first sub - channel is centered at f_s/N.

However, the analysis error of DFT through shifting one sampling clock is as well known almost equal that of shifting maximum $N/2$sampling clocks. This requires digital transmission system restrictly synchronized conditions which is almost impossible in implementations. Even if frames are restrictly synchronized, frequency component blots out the frame during transmitting over radio channel with non linearity to make frame synchronization big problem itself. A new concept of instantaneous spectrum in conquering frame synchronization becomes to be important to solve this big problem.

The frequency component of the instantaneous spectrum corresponding to the first sub - channel of DFT is given by short time DFT(ST DFT) as follows, [5]

$$\widetilde{\phi_1}(n) = \sum_{r=-\infty}^{\infty} \widetilde{h}(n-r)\, x(r)\, e^{-j\frac{2\pi}{N}r} \qquad (9)$$

here, $\widetilde{h}(p)$ is the window function of frequency resolution being f_s/N in ST DFT, for example, given by

$$\widetilde{h}(p) = N\left(\frac{\pi p}{N}\right) K(\beta,\ v)\,. \qquad (10)$$

The length of $\widetilde{h}(p)$ window is given by $-1 \le v \le 1$, that is given by $2mN$. $\widetilde{h}(t)$ defined by eq.10 locates as shown in fig.9 by solid curve with its origin at $n = 0$. The symbol period indicated in the same figure by shade over $(-N/2,\ N/2)$ is equal to that of DFT, which the main frames of the ST DFT, which are corresponding to k_{th} symbol period, locates on the period $(-N,\ N)$ with 50% overlapping among adjacent $k-1$ and $k+1_{th}$ symbol periods.

In order to match the main frames of the ST DFT only to the k_{th} symbol period, window $\widetilde{h}(*)$ is modified as shown in fig.9 by chained curve. This modification causes the enlargement by twice of the sub - channel bandwidth on the frequency domain as shown by shaded zone in fig.10.

It is easy to understand that there exists no problem in enlargement of the sub -

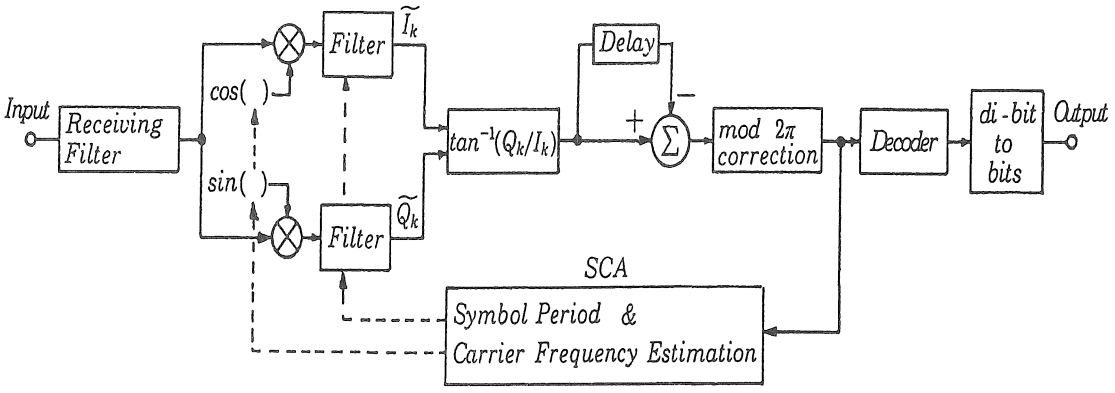

Fig.8 Block diagram of the demodulator.

channel because noise signal on the expanded domain has already eliminated through receiving filter where domains $(0,\ f_m/2)$ and over than $3f_m/2$ are covered by the modified $h(*)$. That is, the instantaneous spectrum given by window $h(*)$ shown by chained curve in fig.9 and given by sub-channel shown by shaded zone in fig.10 is consequently recognized to be given by 0_{th} frequency component of the generalized short time DFT (ST gDFT), [6]

$$\phi_0(n) = \sum_{r=-\infty}^{\infty} h(n-r)\, e^{-j\frac{2\pi}{N}r}, \tag{11}$$

here,

$$h(p) = N\left(\frac{2\pi p}{N}\right) K\left(\beta,\ \frac{2p}{mN}\right), \quad -\frac{mN}{2} \le p \le \frac{mN}{2}. \tag{12}$$

ST gDFT gives strong solutions for yielding I_k and Q_k without any symbol interference distortion, because $h(*)$ given in eq.12 converse into null at every N sampling clock.

6. THEORETICAL PERFORMANCE

Error rate is theoretically evaluated for $\pi/4$-shifted DQPSK on static and Rayleigh fading channel based on the mythology of ref.1. The SER of the differential detector for Gray code with equally probability is given [7].

$$SER = \int_{-\pi}^{\pi} \int_{\theta_1+\Delta\phi+\pi/4}^{\theta_1+\Delta\phi+7\pi/4} P(\theta_2 \mid \phi_2) P(\theta_1 \mid \phi_1) d\theta_2 d\theta_1. \tag{13}$$

The BER is similarly expressed as follows,

$$BER = \int_{-\pi}^{\pi} \int_{\theta_1+\Delta\phi+\pi/4}^{\theta_1+\Delta\phi+5\pi/4} P(\theta_2 \mid \phi_2) P(\theta_1 \mid \phi_1) d\theta_2 d\theta_1. \tag{14}$$

Here, ϕ_i and θ_i, $i = 1, 2$ are the sending true and receiving phase angle of the two successive transmitted symbols, respectively. The phase difference $\Delta\phi = \phi_2 - \phi_1$ is restricted to be $\pi/4 \pm m\pi/2$, $m = 0,\ 1,\ 2,$ where every ϕ_i can take one of values $k\pi/4$, $k = 0,\ 1,\ 2,\ \cdots,\ 7$. $P(\theta_i|\phi_i)$ is the probability density function (pdf) at detecting θ_i after transmitting ϕ_i. When θ_2 is in the range from $\theta_1 + \Delta\theta + \pi/4$ to $\theta_1 + \Delta\phi + 7\pi/4$ one symbol error occurs, i.e. both bits in the symbol are failed in detecting. This double error range is divided into more detailed range in employing Gray coding; single bit error occurs in the two ranges from $\theta_1 + \Delta\phi + \pi/4$ to $\theta_1 + \Delta\phi + 3\pi/4$ and from $\theta_1 + \Delta\theta + 5\pi/4$ to $\theta_1 + \Delta\theta + 7\pi/4$, double bit error occurs in the range from $\theta_1 + \Delta\phi + 3\pi/4$ to $\theta_1 + \Delta\phi + 5\pi/4$. Therefore, single bit error occurs in the range from $\theta_1 + \Delta\phi + \pi/4$ to $\theta_1 + \Delta\phi + 5\pi/4$.

For a static channel, pdf $P(\theta_i|\phi_i)$ is given as

$$P(\theta_i \mid \phi_i) = \frac{1}{2\pi} e^{-2\gamma}\left[1 + \sqrt{8\pi\gamma}\cos(\phi_i - \theta_i)\, e^{2\gamma\cos^2(\phi_i-\theta_i)}\left\{1 - \frac{1}{2} erfc\left(\sqrt{2\gamma}\cos(\phi_i - \theta_i)\right)\right\}\right]. \tag{15}$$

here, erfc is error co-function,

$$erfc(x) = \frac{2}{\sqrt{\pi}} \int_x^{\infty} e^{-t^2} dt.$$

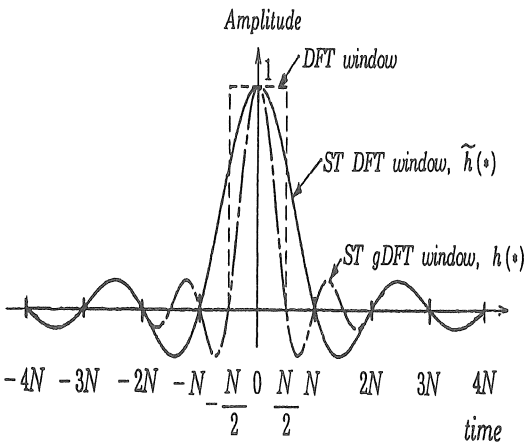

Fig.9 The operand over data stream to show the frame duration.

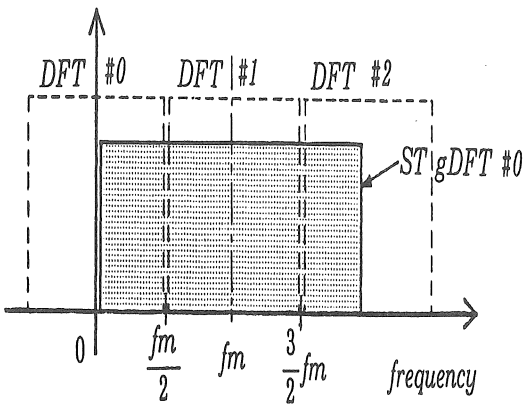

Fig.10 Comparison of the sub-channel allocation between ST DFT and ST gDFT.

For a Rayleigh fading channel, pdf $P(\theta_i|\phi_i)$ is

$$P(\theta_i \mid \phi_i) = \frac{1}{2\pi(1+2\gamma)} + \frac{2}{\pi\gamma}\frac{\cos(\phi_i-\theta_i)}{\left\{4\sin^2(\phi_i-\theta_i)+\frac{2}{\gamma}\right\}^{\frac{3}{2}}} \quad (16)$$
$$\left[\frac{\pi}{2} - \mu(\phi_i,\theta_i) - \frac{1}{2}(2\mu(\phi_i,\theta_i))\right].$$

here,

$$\mu(\phi_i,\ \theta_i) = \tan^{-1}\left\{\frac{-2\cos(\phi_i,\ \theta_i)}{\sqrt{4\sin^2(\phi_i-\theta_i)+\frac{2}{\gamma}}}\right\} \quad (17)$$

and γ denotes SNR given as

$$\gamma = \frac{E_b}{Nf_\omega}\int_{f_1}^{f_2} H^2(f)\,df, \quad (18)$$

where $H(f)$ is frequency response of the matched filters $f_\omega = f_2 - f_1$, and f_2 or f_1 means lower or upper edge of the pass-band.

As shown in eq.18, SNR and error rate are improved if the matched filter power is concentrated into passband. Figure 6.1 shows these theoretical results. In a static channel, the error rate is improved exponentially if SNR goes large linearly. On the other hand, the error rate is improved by only one figure if SNR increases by 10 dB in a Rayleigh fading channel. The Nyquist Kaiser filter discussed in the later session improves remarkably the error rate as shown by chained curves in a static channel and has the trend of improving the error rate if its parameter β goes large on the base of power being concentrated towards to the center frequency.

7.SIMULATION RESULTS

The ST gDFT demodulator has employed in simulations to confirm the efficiency being more than 1.80 bit/Hz. The RC filter, with a roll-off factor of 0.35 and truncated to 8 symbol period, was used as both sending and receiving filter to compose conventional matched filter system as shown in figs.2 and 8. The ST DFT filter, with β =4.313 and truncated to the same length by 8 symbol, is employed for each filter of the matched filter system of the proposing system.

BER performance was determined by using Monte Carlo simulation procedure. Each simulation was carried over 5,000 frames of data and averaged over 4 independent runs.

Figure 11 also shows theoretical and simulation results of BER and SER vs. Eb/No for a static and Rayleigh fading

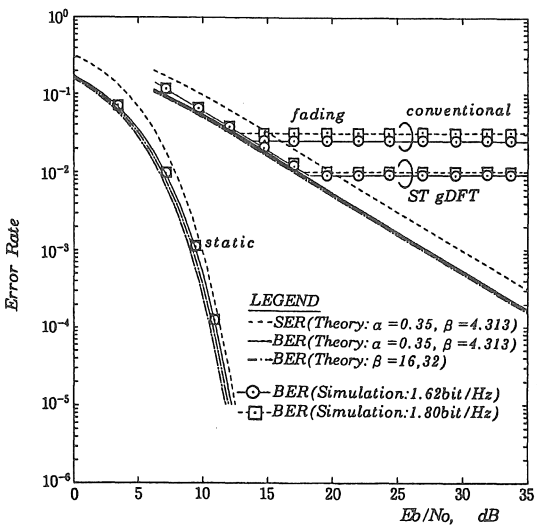

Fig.11 Error performance in a static and Rayleigh fading channel.

channel. This figure also shows that SER is almost twice by BER, as is expected with Gray coding. It is observed that the BER in Rayleigh fading is approximately equal to $0.5(Eb/No)^{-1}$ for Eb/No larger than 10dB. The BER of the ST gDFT system for efficiently 1.80 bit/Hz is saturated to 1.0×10^{-2} in the fading to be more improved by 4.9dB than conventional system.

8. CONCLUSION

The generalized Short Time DFT has successfully discussed with emphasis on ST gDFT demodulator which is able to reduce error rate by genius desmearing function, and on Nyquist Kaiser which is suit well to matched filter to prevent from inter symbol interference.

It is shown that $\pi/4$-shifted DQPSK can transmit at a high efficiency 1.80 bit/Hz with employing Nyquist Kaiser filter and ST gDFT demodulator. The author would like to thank the students of Kishi Lab. at AIT for their assistant in simulations.

REFERENCES

[1] S.Chennakeshu and G.J.Saulnier, "Differential Detection of $\pi/4$-Shifted DQPSK for Digital Cellular Radio", IEEE VTC'91, St.Louis, Missouri, pp.186-191, May 1991.

[2] Jenks,F.J., Morgan,P.D., and Warren,C.S.,"Use of four-level phase modulation for digital mobile radio", IEEE Trans. Electromagn. Compat., Vol.EMC-14, pp.113-128, Nov. 1972.

[3] Carlson, a.b., "Communication Systems; An Introduction to Signal and Noise in Electrical Communication", 2nd ed., McGraw-Hill Book Co., New York, 1975

[4] W.C.Jakes, "Microwave Mobile Communications", John Wiley & Sons, New York, 1974.

[5] M.Kishi, "A Proposal of Short Time DFT Hilbert Transformers and Its Configuration", Trans. IEICE, Vol. E71, No. 5, pp.466-468, May 1988

[6] M.Kishi, T.Ishiguro, and Y.Kozaki, "Application of the Generalized Short Time DFT to the Hilbert Transformer and Its Characteristics", IEEE VTC'93, Secaucus, New Jersey, (in this conference)

[7] S.Ono, N.Kondoh, and Y.Shimazaki, "Digital Cellular System with Liner Modulation", Proc. of the IEEE VTC, Vol.1, pp.44-49, May 1989, San Francisco, California.

(受理 平成6年3月20日)